Valence charge density in grey tin: X-ray determination of the (222) "forbidden" reflection and its temperature dependence*

D. H. Bilderback and R. Colella
Department of Physics, Purdue University, West Lafayette, Indiana 47907
(Received 5 August 1974)

The (222) reflection of diamondlike lattices is essentially contributed at room temperature by valence electrons piled up between neighboring atoms. It is therefore a direct experimental proof of the existence of covalent bonding charges in diamond structures. Such a proof has now been established in the case of grey tin. The (222) reflection has been measured in absence of simultaneous reflections on an absolute basis, using Cu $K\alpha$ radiation. Its intensity is four orders of magnitude smaller than the (333), corresponding to a structure factor $F_{222} = 1.06 \pm 0.05$ electrons/cell at 200°K. This value is 52% smaller than that calculated using a pseudopotential approach. Similar measurements were repeated at different temperatures between 80 and 223 °K. The nuclear mean-square vibrational amplitude was found to be 0.0319 ± 0.002 Å^2 at 200 °K, very close to the value obtained from lattice-dynamics calculations, corresponding to a Debye temperature of 150 °K. The temperature dependence of the valence bonding charges suggests, however, that their mean-square vibrational amplitudes may be some 20% smaller than that of the core.

I. INTRODUCTION

Grey tin is the heaviest element which crystallizes in the diamond crystal structure, and marks the transition from covalent to metallic in the IV column of the Periodic Table. It is a semiconductor with an extremely small energy gap. As a matter of fact, the top of the valence band touches the bottom of the conduction band at $\vec{k} = 0$, which puts this crystal in the particular class of the so-called zero-gap semiconductors. The average energy gap is not zero, but it is probably the smallest one among all tetrahedrally coordinated semiconductors (3.06 eV). Since the average energy gap represents the difference between the bonding and antibonding energy levels, one is led to conclude that directional bonding should not be very pronounced in grey tin, a natural trend as the core size is increased. In fact, the next element in the fourth group is lead, a close-packed metal. It is therefore interesting to gain some information about the valence-electron charge density of grey tin, in order to assess the covalent character of its bonding. The most direct experimental proof of tetrahedral deformation in diamond structures is offered by the weak nonzero (222) x-ray forbidden reflection,[1] which is mostly contributed by valence electrons.

The vibrational properties of these valence electrons have been the subject of recent intensive investigations, in the case of Ge and Si.[2,3] According to the shell model one would expect that the valence electrons vibrate with less amplitude than the ions.[2] A substantially reduced temperature dependence for the valence electrons in Si is also predicted by the bond-charge model, in which the interstitial covalent charge is related to the static dielectric constant and therefore to the index of refraction.[4] Experimental observations described in Refs. 2 and 3 do not seem to support this hypothesis, although Fujimoto's work[2] shows that the mean-square vibrational amplitude of the valence electrons in Si may be 10% smaller than that of the core. One of the problems in interpreting the Si and Ge data is the presence of anharmonicity in the thermal motion of the core at high temperatures. In the case of grey tin one is limited to a low-temperature region because the crystal transforms to white tin at 13.2 °C. While this limitation restricts our temperature range, the fact the anharmonicity is negligible at low temperatures simplifies considerably the interpretation of the experimental data.

II. EXPERIMENTAL

Grey-tin single crystals were grown in a saturated mercury solution at −30 °C by Ewald and co-workers.[5] Most of the crystals had several perfect mirrorlike (100) and (111) faces. Therefore, it was not necessary to cut, polish, and etch the crystals. The samples were stored below 0 °C at all times to keep the mercury from combining with the grey tin. The crystal orientation was easily determined after identifying the hexagonal faces as (111) and the rectangular natural faces as (100). Back-reflection Laue photographs confirmed these orientations. A perfect-looking (111) crystal was selected and the backside tip end of the crystal was frozen with mercury to a copper cup and mounted in a low-temperature cryostat. During handling the crystal was cooled with dry ice and a light frost was cleared from the crystal by cleaning with

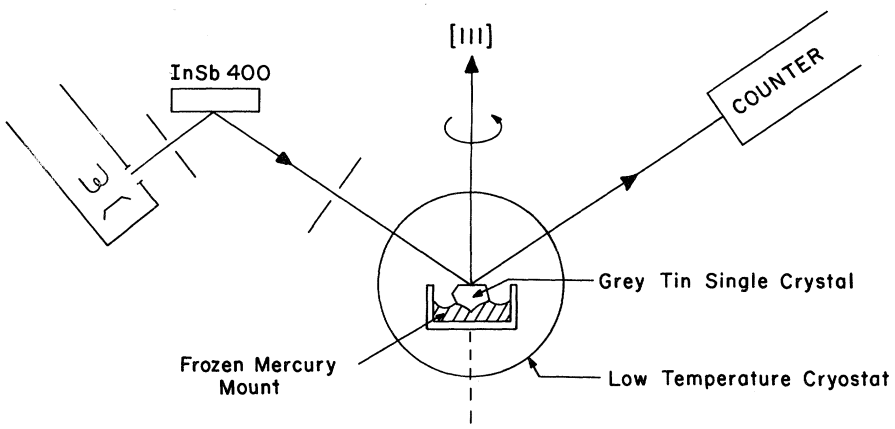

FIG. 1. Double-crystal arrangement for measuring the (222).

methyl alcohol cooled to −40 °C.

A double crystal spectrometer (Fig. 1) was used to measure the integrated intensities. A perfect InSb (400) first crystal provided close matching ($\theta_B^{400} = 28.4°$) to the (222) grey tin crystal ($\theta_B^{222} = 24.3°$). Copper radiation ($\lambda = 1.54$ Å) yielded favorable *Umweganregung*-free regions. A stabilized x-ray generator operating at 45 KV and 30 mA kept the direct beam stable to within 1% after correcting for changes in atmospheric pressure. Four calibrated brass foils, each attenuating the direct beam by a factor of 8, were used to place the direct beam intensity measurements on an absolute basis. The direct beam intensity was 8.4×10^5 counts/sec when measuring the (222). The slit system allowed a beam 0.7 mm wide and 2 mm high to fall upon the grey tin crystal. A single channel analyzer set for the $K\alpha$ peak rejected the harmonic contaminant of $\frac{1}{2}\lambda$ from the proportional counter. An electronic background of 0.06 counts/sec was present in our measurements.

A scan interval of four times the α_1-α_2 spacing was selected. Increasing the angular interval showed a negligible increase ($\lesssim 1\%$) in the integrated intensity. The background was counted at both extremities and subtracted from the total intensity.

All measurements were made at an *Umweganregung*-free azimuth (arrow, Fig. 2). The cryostat could be rotated by ±5° around the [111] direction and therefore the azimuthal alignment could be completed by locating some peaks due to multiple diffraction in the diffracted (222). The peaks were identified with the aid of a computer-predicted *Umweganregung* pattern and carefully avoided. A typical (222) rocking curve is shown in Fig. 3.

The small crystal size (4×2.5 mm) made the horizontal alignment difficult. Two methods were used to ensure that the incident beam completely hit the crystal. In the first method a neighboring *Umweganregung* peak was excited to produce a strong (222) diffracted intensity. Lead slits were placed before and after the grey tin crystal to sharply define the path of the x rays. The proportional counter was replaced with a He-Ne laser

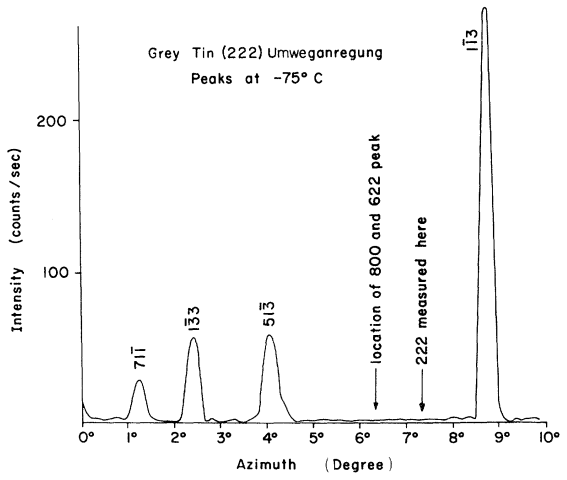

FIG. 2. *Umweganregung* pattern at the (222) diffracting position. The 0° azimuth corresponds to a position in which the [1$\bar{1}$0] axis lies in the diffraction plane, forming an angle less than 90° with the incident beam. The (800) and (622) do not produce any appreciable *Umweg* peak.

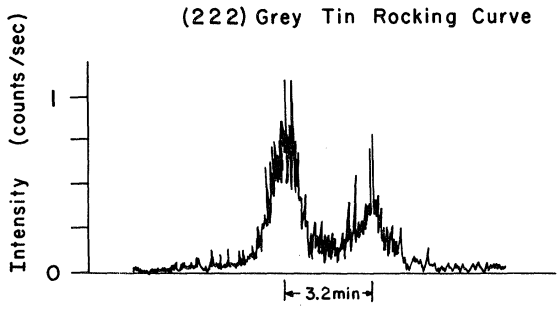

FIG. 3. Typical (222) rocking curve. The two peaks correspond to $K\alpha_1$ and $K\alpha_2$.

adjusted to retrace the path of the x rays through the slit system. The laser beam then clearly marked out the diffracting region of the crystal for visual observation.

The second method involved translating the crystal forward and backward along the [111] direction (Fig. 1) to discover, with some care, the left and right edges of the crystal. For the final measurements, the sample was surrounded with five turns of "superinsulation" (aluminized Mylar) to minimize radiation losses to the outer radiation shield at 80 °K. About 6% of the intensity was lost due to the superinsulation and the horizontal alignment was performed by the second method.

The error bars on the (222) (Fig. 4) correspond to ±3% and were estimated from statistics and experimental reproducibility. The experimental values for the (222) and (444) integrated intensitites as a function of temperature were quite linear over the temperature range examined. Hence it was not necessary to plot the log of the integrated intensity against a reduced temperature. This point was checked by comparing with calculated I-vs-T plots (I is the integrated intensity), using dynamical theory for the (444) and kinematical theory for the (222). A least-squares straight-line fit to the (444) experimental data yielded a slope consistent with a Debye temperature of $\Theta_M = (150 \pm 5)$°K. This value corresponds to a mean-square vibrational amplitude $\langle u^2_{\text{core}} \rangle = 0.0319$ Å^2 at 200 °K, whereas a least-squares fit to the (222) data yields $\langle u^2_{\text{bond}} \rangle = 0.0250$ Å^2 at the same temperature.

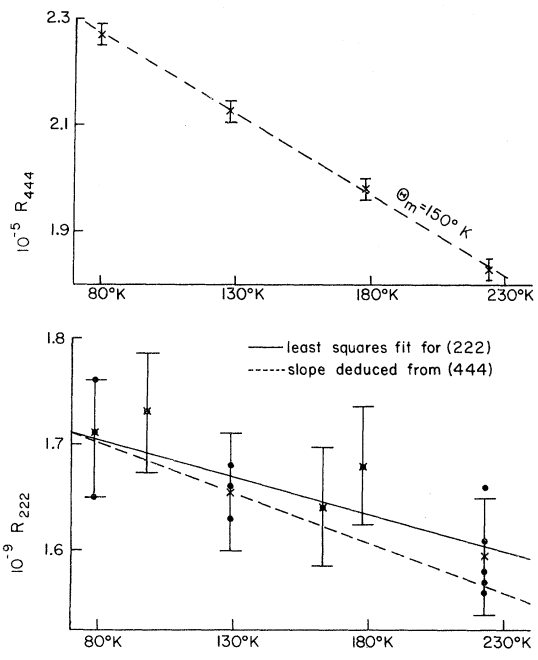

FIG. 4. Integrated intensities as a function of temperature for (222) and (444). Dots denote a single measurement and the crosses are the average of all the dots at a particular temperature. The dashed lines have a slope consistent with $\Theta_M = 150$ °K.

III. DISCUSSION

The (333) and (444) reflections were close to the dynamical values, an indication of good crystal perfection. Table I summarizes our results and shows the comparison between observed and calculated values. A Debye temperature of 150 °K was used in the calculations, as determined from the temperature dependence of the (444).

This value of Θ_M is appreciably different from Θ_D, the Debye temperature deduced from specific-heat measurements at low temperature[6]: $\Theta_D = 260$ °K. There is good agreement, however, with the value calculated from the dispersion curves obtained by neutron inelastic scattering[7]; $\Theta_M^{\text{calc}} = 153$ °K. This indicates that grey tin is not a Debye solid. A similar phenomenon has been observed for Ge and Si.[8]

The scattering factors and the anomalous dispersion corrections were taken from Refs. 9 and 10, respectively. The (222) reflection is very weak and the dynamical and kinematical values agree within less than 1%; therefore kinematical theory was used for calculating F_{222} from integrated intensity data. A possible contribution to the (222) from anharmonic vibrations, predicted theoretically[11] and experimentally observed in Ge and Si,[12,13] was evaluated for grey tin using the treatment given in Ref. 11 with a value for the thermal expansion coefficient of 4.7×10^{-6}/°C. Such a contribution turned out to be less than 2% at the highest temperature of interest and was neglected in the subsequent analysis.

A convenient explanation for a nonzero (222) structure factor in diamond structures can be given in terms of a tetrahedral deformation of the charge density[14]:

$$\rho = (1/4\pi)[1 \pm \alpha xyz/(x^2+y^2+z^2)^{3/2}]^2 R^2, \qquad (1)$$

where α is an adjustable parameter and R^2 is the

TABLE I. Experimental and theoretical integrated intensities. The calculations were based upon both dynamical and kinematical theories using $\Theta_M = 150$ °K and a crystal temperature of 200 °K.

hkl	R^{calc}_{hkl} Dynamical theory	R^{expt}_{hkl}	R^{calc}_{hkl} Mosaic theory
222	...	1.62×10^{-9}	...
333	1.38×10^{-5}	1.53×10^{-5}	2.27×10^{-5}
444	1.65×10^{-5}	1.91×10^{-5}	2.74×10^{-5}

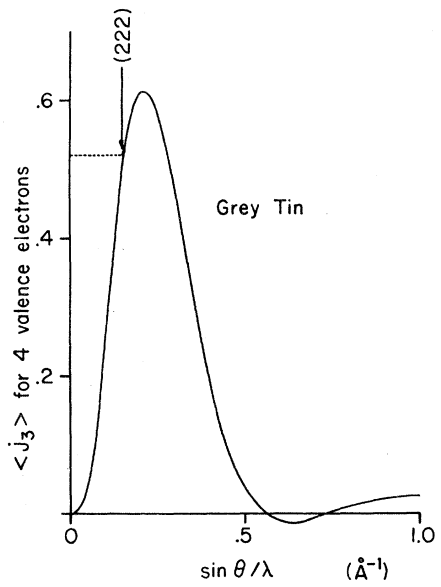

FIG. 5. Plot of $\langle j_3 \rangle$ for the four valence electrons of grey tin.

radial part of the valence charge density. In our calculations R^2 was contributed by the $5P^2$ and $5S^2$ radial wave functions. The extra term in parentheses has the same site symmetry ($\bar{4}3m$) of the atomic positions and introduces "lobes" extending toward nearest neighbors. The scattering factor can be evaluated from (1) in terms of α, hkl and terms like $\langle j_n(k) \rangle$ where $k = 4\pi \sin\theta/\lambda$ and

$$\langle j_n(k) \rangle = \int_0^\infty r^2 R^2 j_n(k) dr ,$$

where $j_n(k)$ is the n-th spherical Bessel function. In the case of F_{222} only $\langle j_3(k) \rangle$ is involved and its value was evaluated using Hartree-Fock wave functions.[15] A plot of $\langle j_3(k) \rangle$ as a function of $\sin\theta/\lambda$ is presented in Fig. 5. The value of α deduced from our measurements at 200 °K is $\alpha = 0.64$ and Fig. 6 shows the effect on the charge density along [111] between two nearest neighbors. It is seen that an appreciable increase in the central region is obtained, in qualitative agreement with the value predicted by pseudopotential theory.[16] The F_{222} value calculated from such a theory[17,18] ($F_{222} = 2.22$) is considerably greater, however, than the measured value, which seems to indicate that an extra contribution to F_{222}^{calc} is given by the pseudocharge density close to the cores, where the discrepancy between Hartree-Fock and pseudo-wave functions is more evident.

The temperature dependence of the (222) is shown in Fig. 4 and does not seem to be very different from that of the core, as deduced from the (444), although a least-squares analysis of several measurements indicates a mean-square vibrational amplitude for the bonding electrons $\langle u_{\text{bond}}^2 \rangle$ that is 22% smaller. The scattering of our data, corresponding to a percentage error in the slope of ±20%, makes it questionable to what extent this

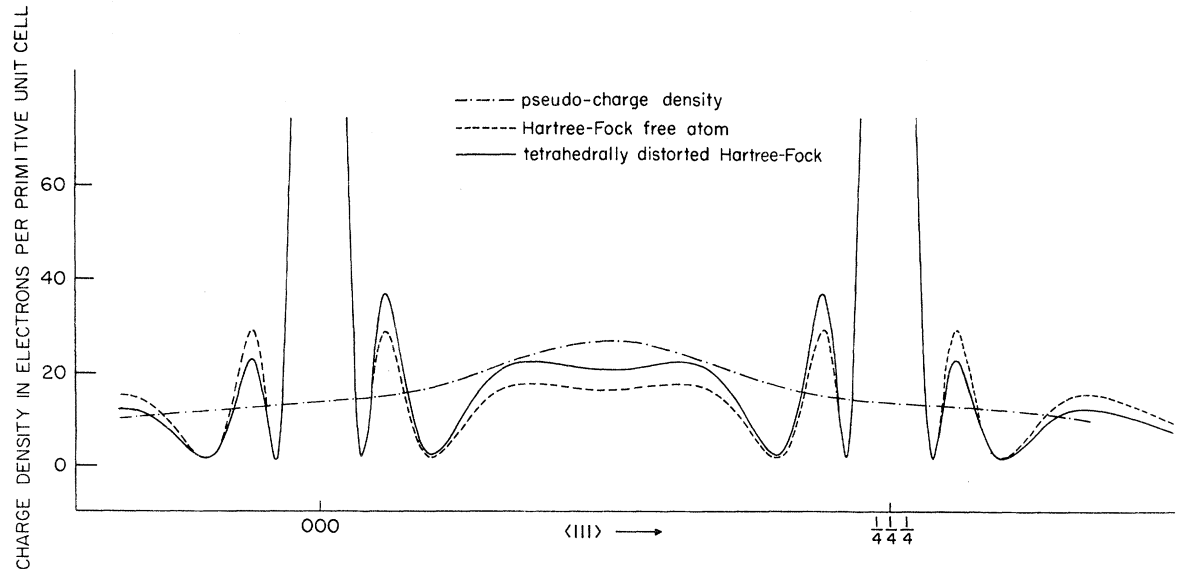

FIG. 6. Valence charge density plotted along the [111] direction, between two nearest neighbors located at 0 0 0 and $\frac{1}{4}\frac{1}{4}\frac{1}{4}$. The dotted line corresponds to Hartree-Fock (free-atom) wave functions. The dashed line is obtained from a pseudopotential calculation (see Fig. 20 in Ref. 16). The solid line is based on tetrahedrally distorted Hartree-Fock wave functions. The oscillations of the solid and dotted lines near the cores have been neglected.

difference is meaningful. Furthermore, the value of $\langle u^2_{\text{core}} \rangle = 0.0319$ Å^2 was deduced using dynamical theory, that is to say, e^{-M} dependence. If the (444) is not completely dynamical, as Table I seems to suggest, its temperature dependence may be steeper than e^{-M}, thereby corresponding to a smaller $\langle u^2_{\text{core}} \rangle$. Shell-model calculations of the mean-square vibrational amplitudes for the bonding charges in Si (Ref. 2) predict a value which is 26% smaller than that of the core, but the experimental observations[2-3] are in favor of a much smaller difference. In the case of grey tin we draw essentially the same conclusions valid for Ge and Si, that is to say, the thermal motion of the bonding charges looks essentially the same as that of the core, or, at most, it may be about 20% smaller.

IV. CONCLUSIONS

The "forbidden" (222) reflection has been measured with x rays in grey tin single crystal and found to be $F_{222} = 1.06 \pm 0.05$ at 200 °K. The existence of this nonzero forbidden reflection is a direct experimental proof of tetrahedral distortion of the valence electrons in this narrow-gap semiconductor. This result has been interpreted in terms of a phenomenological model of the charge density in which the tetrahedral distortion is introduced by means of a nonspherical term with local tetrahedral symmetry and over-all cubic symmetry. In this way the charge density between nearest neighbors is appreciably increased over the free-atom value, in qualitative agreement with pseudopotential calculations. The F^{calc}_{222} pseudo-structure-factor, however, is almost twice the experimental value, which is probably due to the extra pseudo-charge present near the cores.

The temperature dependence of (222) and (444) has been determined between 80 and 223 °K. The latter reflection has been used for determining the Debye temperature Θ_M, which turned out to be 150 °K, appreciably lower than Θ_D deduced from specific heat (260 °K) but in good agreement with the value calculated from inelastic neutron scattering data. The temperature dependence of the (222) indicates a mean-square vibrational amplitude of the bonding charges equal to 0.78 $\langle u^2_{\text{core}} \rangle$, with an experimental uncertainty of ±20%.

ACKNOWLEDGMENTS

The authors are thankful to Professor A. W. Ewald of Northwestern University who kindly provided a generous supply of grey tin single crystals. Thanks are also due to Dr. J. B. Mann of Los Alamos Scientific Laboratory who sent us a tape with the Hartree-Fock wave functions, and to Professor J. P. Walter for the calculation of the (222) structure factor from pseudo-charge-density data.

---

*Work supported by the National Science Foundation Materials Research Laboratory Grant No. GH33574 and by National Science Foundation Grant No. GH39200.

[1] W. H. Bragg, Proc. Phys. Soc. Lond. 33, 304 (1921).
[2] I. Fujimoto, Phys. Rev. B 9, 591 (1974).
[3] J. B. Roberto, B. W. Batterman, and D. T. Keating, Phys. Rev. B 9, 2590 (1974).
[4] J. C. Phillips, Phys. Lett. A 37, 434 (1971).
[5] A. W. Ewald and O. N. Tufte, J. Appl. Phys. 29, 1007 (1958).
[6] R. W. Hill and D. H. Parkinson, Philos. Mag. 43, 309 (1952).
[7] G. Dolling (private communication).
[8] B. W. Batterman and D. R. Chipman, Phys. Rev. 127, 690 (1962).
[9] D. T. Cromer and J. B. Mann, Acta Crystallogr. A 24, 321 (1968).
[10] D. T. Cromer, Acta Crystallogr. 18, 17 (1965).
[11] B. Dawson and B. T. M. Willis, Proc. R. Soc. Lond. A 298, 307 (1967).
[12] D. T. Keating, A. Nunes, B. W. Batterman, and J. Hastings, Phys. Rev. B 4, 2472 (1971).
[13] J. B. Roberto, B. W. Batterman, and D. T. Keating, Phys. Status Solidi B 59, K59 (1973).
[14] R. J. Weiss, Phys. Lett. 12, 293 (1964).
[15] J. B. Mann, Los Alamos Scientific Laboratory, 1968 (unpublished).
[16] J. P. Walter and M. L. Cohen, Phys. Rev. B 4, 1877 (1971).
[17] J. P. Walter (private communication).
[18] M. Jaroš and P. K. W. Vinsome, Phys. Lett. A 33, 350 (1970).